Am J Cancer Res 2024;14(4):1730-1746
www.ajcr.us /ISSN:2156-6976/ajcr0155114

Original Article

Circular RNA circIL21R promotes cervical cancer cells proliferation and migration by sponging the miR-1205/PTBP1 axis

Zhuoqun Ma[1,2], Haofeng Zhang[1], Yaqin Wang[1], He Zhao[1], Yanan Li[3], Jun Zhang[1], Xiaohui Xu[1]

[1]Department of Obstetrics and Gynecology, Beijing Anzhen Hospital Affiliated to Capital Medical University, Beijing 100011, China; [2]Department of Gynecology, University Medical Center Hamburg-Eppendorf (UKE), Hamburg 20246, Germany; [3]Department of Oncology, The First Medical Center, Chinese PLA Key Laboratory of Oncology, Key Laboratory for Tumor Targeting Therapy and Antibody Drugs, Chinese PLA General Hospital, Beijing 100853, China

Received December 25, 2023; Accepted March 15, 2024; Epub April 15, 2024; Published April 30, 2024

Abstract: Increasing research has shown that the abnormal expression of circRNAs is closely related to tumorigenesis, apoptosis, and patient prognosis in cervical cancer. This study aimed to reveal the procancer role of circIL21R in cervical cancer and investigate its related molecular mechanisms. Bioinformatics analysis revealed that circIL21R promotes the progression of cervical cancer via the miR-1205/PTBP1 axis. CircIL21R expression was significantly greater in tumor tissue than in adjacent normal tissue, and higher circIL21R expression indicated shorter survival. We applied MTS assays, EdU assays, and Transwell assays to show that the overexpression of circIL21R promoted cervical cancer cell proliferation and invasion. Mechanistically, circIL21R promoted the expression of PTBP1 by sponging miR-1205. Moreover, rescue assays confirmed that regulating the expression of miR-1205 or PTBP1 could reverse the tumorigenic effect caused by circIL21R overexpression. In addition, circIL21R promoted the tumorigenesis of cervical cancer in vivo. In summary, our study demonstrated that circIL21R was highly expressed in cervical cancer and upregulated PTBP1 expression by acting as a ceRNA for miR-1205, making outstanding contributions to several malignant biological processes in cervical cancers, such as growth, proliferation, and invasion. CircIL21R is a potential biomarker for the diagnosis and treatment of cervical cancer.

Keywords: Cervical cancer, circIL21R, miR-1205, PTBP1, proliferation

Introduction

According to the International Agency for Research on Cancer, cervical cancer has the fourth highest incidence and mortality rate globally [1]. The latest statistics show that 604,127 new cases of cervical cancer and 341,831 deaths occurred in women worldwide in 2020, accounting for 6.5% and 7.7% of the total female cancer incidence and deaths, respectively [2]. The occurrence and progression of cervical cancer involve a combination of viral infection, multiple abortions, long-term use of contraceptives, and other factors [3, 4]. In addition, numerous studies have identified persistent infection with high-risk human papillomavirus as a critical risk factor for the development of cervical lesions and cervical cancer tumors [5, 6]. In recent years, despite many advances in the standard treatment of surgery combined with radiotherapy or chemotherapy, treatment outcomes are still unsatisfactory. More than 80% of cervical cancer deaths are now caused by tumor metastasis and invasion [7]. Therefore, a more in-depth exploration of the molecular mechanisms of cervical cancer invasion and metastasis and the development of new therapeutic targets will greatly benefit cervical cancer screening, early diagnosis, the development of more appropriate treatment plans, and the improvement of prognosis [8].

Circular RNAs (circRNAs) are a new class of endogenous noncoding RNAs (ncRNAs) that are hundreds to thousands of nucleotides in length and are more stable than linear RNAs. CircRNAs form a covalently closed loop by reverse splicing without the 5' and 3' ends of traditional lin-

ear RNA [9, 10]. With increasing research, abnormal expression of circRNAs has been associated with tumor progression. It is closely related to tumorigenesis, apoptosis, clinical staging, and patient prognosis. Previous studies have shown that circRNAs regulate the invasion and metastasis of cervical cancer. For example, circ0000069 expression is upregulated in cervical cancer cells and tissues, and circ0000069 promotes the proliferation and migration of cervical cancer cells [11]. Circ_0003221 acted as a sponge of miR-758-3p to upregulate CPEB4 [12]. Circ_0000730 inhibits cervical cancer cell proliferation, migration, and invasion by regulating the miR-942-5p/PTEN axis. Circ_0000730 may play an oncogenic role in cervical cancer and may be a candidate target for treating cervical cancer [13].

In this study, bioinformatics analysis revealed that circIL21R (circBase ID: hsa_circ_0038728, chr16:27445667-27449008) was significantly more highly expressed in cervical cancer tissues than in normal tissues and was associated with patient survival time. We also tested the expression level of circIL21R in clinical specimens, and the results corroborated the conclusions drawn from bioinformatics analysis. There are no reports on the procancer effects of circIL21R in cervical cancer. Therefore, this study aimed to reveal the procancer role of circIL21R in cervical cancer and investigate its related molecular mechanisms.

To explore in-depth the role and detailed biological mechanisms of circIL21R in the progression of cervical cancer malignancy, we conducted a bioinformatics analysis. The results showed that circIL21R promotes the progression of cervical cancer through the miR-1205/PTBP1 axis. MicroRNAs (miRNAs) are a class of small noncoding single-stranded RNAs of approximately 18-25 nt in length that are involved in various physiological and pathological processes in the body. It can regulate target genes and signaling pathways and is widely related to the biological behaviors of cells [14]. miRNAs are found in various body fluids and are especially widespread and stable in serum. miRNAs are closely related to the proliferation, apoptosis, and invasion of cancer cells [15]. The regulatory role of miR-1205 in different tumor types has been extensively researched. In ovarian, breast, osteosarcoma, and rectal cancers, miR-1205 promotes the malignant phenotype of the tumor. The downregulation of expression is due to the competing endogenous RNA mechanism [16-19]. However, the role of miR-1205 in cervical cancer has yet to be further investigated. In our research, miR-1205 was shown to directly regulate the RNA-binding protein (RBP) polypyrimidine tract-binding protein 1 (PTBP1) to modulate the progression of cervical cancer cells [20]. Therefore, this study aimed to analyze the expression levels of circIL21R, miR-1205, and PTBP1 in cervical cancer, revealing the role and regulatory mechanism of circIL21R in the malignant progression of cervical cancer.

Materials and methods

Patient samples and ethic

We collected fresh cervical cancer tissue from 18 patients hospitalized and surgically treated at the Department of Obstetrics and Gynecology, Beijing Anzhen Hospital from 2018 to 2023. All excised or biopsied specimens were immediately placed in liquid nitrogen and stored at -80°C. According to the World Health Organization (WHO) classification guidelines, two pathologists confirmed the histological diagnosis. None of the patients had received chemotherapy, radiotherapy, or adjuvant treatment prior to surgery. Basic information on the patients, clinical indicators, and pathology was also collected sufficiently. The age of the patients ranged from 29 to 71 years with a median age of 53 years. Only squamous cell carcinoma samples were included in this study. There were 11 cases of stage I-IIa, 4 cases of stage IIb, and 3 cases of stage IIIa based on the International Federation of Gynecology and Obstetrics criteria. The Capital Medical University Ethics Committee approved this research, and all subjects finished written informed consent.

Cell culture and cell transfection

The Cell Bank of the Chinese Academy of Sciences (Shanghai, China) provided human cervical cancer cell lines (ME180, C33A, Caski, and SiHa). Cell culture was performed at 37°C in a 5% CO_2 humidity incubator using Roswell Park Memorial Institute 1640 medium supplemented with 10% fetal bovine serum (Gibco, Gaithersburg, MD, USA) and 100 U/ml penicillin

and 100 mg/ml streptomycin (Thermo Fisher Scientific, Waltham, MA, USA).

pCD5-ciR vector (Geneseed, Guangdong, China) was used to structure the overexpression plasmid and the control group of circIL-21R. Geneseed (Guangdong, China) designed the sequences of siRNA targeted to circIL21R and PTBP1 to knockdown: circIL21R-KD: 5'-GAGCAGCTGGGGCTGCCCCGA-3'; PTBP1-KD: 5'-TCGCATTCTTTCCGTTTTCCTGA-3'. The mimics and inhibitor reagents of miR-1205 and corresponding negative controls were purchased from Thermo Fisher Scientific (ID: MC13578, MH13578). Transfections were conducted by Lipofectamine 2000 reagent (Invitrogen, Carlsbad, CA, USA) based on the protocol of the manufacturer.

RNase R

RNase R assays validated the circular form of circIL21R. Briefly, 10 μg RNA was extracted from the cell lines and incubated with RNase R (Sigma, Santa Clara, CA, USA) or not for 1 hour at 37°C. Then qRT-PCR was used to test the relative expression of circIL21R and IL21R mRNA.

Quantitative real-time PCR (qRT-PCR)

Trizol reagent (ThermoFisher) extracted RNA from cervical cancer tissues and cell lines. Prime-Script RT Master Mix (TaKaRa, Kyoto, Japan) synthesized cDNA to analyze circRNAs and mRNA, or miRNAs. qRT-PCR (Roche LightCycler480, Roche Diagnostics, Basel, Switzerland) detection using Master Mix SYBR Green (Yeasen Biotechnology, Shanghai, China). Correlated expression was calculated using the Using 2-ΔΔCt method. β-actin was performed as the control. The primers of miR-1205 were purchased from Thermo Fisher Scientific (Primer ID: Hs00508322_CE). Sequences of primers show here as circIL21R, forward 5'-ACTTCATGGCCGACGACATT-3' and reverse 5'-CCGTCTGGAGGTAATCGGTG-3'; PTBP1, forward 5'-AGCGCGTGAAGATCCTGTTC-3' and reverse 5'-CAGGGGTGAGTTGCCGTAG-3'; β-actin, forward 5'-CATGTACGTTGCTATCCAGGC-3' and reverse 5'-CTCCTTAATGTCACGCACGAT-3'.

Fluorescence in situ hybridization (FISH)

To locate circIL21R in cell lines, we designed oligonucleotide probes with fluorescent labels that are complementary to circIL21R junction sequences using the Clone Manager suite. A total of 1×10^5 cells was cultured on a confocal dish overnight at the temperature of 37°C with the 5% CO_2 condition. Subsequently, a specific circIL21R FISH kit (BersinbioTM circRNA FISH, Guangzhou, China) was used to perform the RNA FISH assay according to the protocols of manufacturers. 4,6-diamidino-2-phenylindole (DAPI, Thermo Fisher Scientific) was used to label nuclei. Photographs were acquired by a confocal microscope (Olympus, Tokyo, Japan).

Nuclear-cytoplasmic fraction assay

The RNA was isolated from the nucleus and cytoplasm of cell lines using an RNA Subcellular Isolation Kit (Active Motif, Carlsbad, CA, USA) and TRIzol (Invitrogen). Subsequently, qRT-PCR was performed to evaluate the ratio of nuclear to cytoplasmic distribution. GAPDH and U6 (Abcam, Cambridge, UK) were selected as the internal control for cytoplasmic and nuclear respectively.

Western blot

RIPA lysis buffer (Beyotime Biotechnology, Shanghai, China), which contains PMSF and protease inhibitor, was used to collect and lyse cells. We used BCA protein assay kits (Beyotime Biotechnology) to test the total protein concentration. 40 μg of each protein sample were separated by 12% SDS-PAGE before transferring to PVDF membranes (Invitrogen). Non-fat milk was used in the blocking procedure, and the indicated primary and secondary antibodies were used to detect target protein expression. Antibody against PTBP1 (ab133734) and β-actin (ab8226) was purchased from Abcam.

MTS proliferation assay

MTS assays were performed as a previous report [21]. The CellTiter 96 Aqueous non-radioactive cell proliferation detection kit (Promega, Madison, WI, USA) was used to evaluate the proliferation of cervical cancer cell lines. An ultraviolet spectrophotometer (Thermo Fisher Scientific) measured the absorption at 495 nm.

5-Ethynyl-2'-deoxyuridine (EdU) proliferation assay

Cervical cell lines were seeded in 24-well plates for 24 h at 37°C, and the density was 1×10^5

cells per well. After that, add EdU reagents (Vazyme Biotech, Nanjing, China) for 2 hours. Paraformaldehyde was chosen to fix the cell lines. Positive cells were visualized, and images were captured via a laser scanning microscope (Olympus).

Transwell assay

Dilute Matrigel (Thermo Fisher Scientific) by chilled serum-free growth medium to the density of 20%. Then place 100 μl diluted Matrigel at the center of the 24-well plate upper chamber before incubating for 2 h at 37°C with 5% CO_2. The upper chamber contained the serum-free growth medium. In contrast, the lower chamber contained a 600 μl medium with 10% fetal bovine serum. Cells in the upper chamber were removed, and PBS washed the cells in the lower chambers after one day incubated at 37°C for 24 h. Methyl alcohol fixed cells for 30 minutes, stained with crystal violet for 15 minutes, and then imaged and counted by microscope.

Luciferase activity analysis

In brief, wild-type circIL21R, mutant circIL21R, wild-type PTBP1, and mutant PTBP1 were cloned to the pmirGLO-derived vectors (Invitrogen). 24-well plates were used to seed the cervical cell lines. Luciferase activity was detected via a Dual-Luciferase Reporter Assay System (Invitrogen Promega) following the protocol of the producers. The value of Renilla normalized the luciferase activity.

RNA immunoprecipitation (RIP) assay

We used EZ-Magna RIP RNA-binding Protein Immunoprecipitation Kit (Merck Millipore, Darmstadt, Germany) to conduct RIP assays. Briefly, cell lines were lysed by ice-cold lysis buffer with RNase and protease inhibitors after harvesting. The Antibodies against Ago2 (Merck Millipore) or normal mouse IgG and protein A/G magnetic beads were administrated to the lysates before incubating overnight at 4°C with gentle rotation. Then we washed away the magnetic beads. After that, we eluted and extracted the precipitated RNAs on beads. Finally, the expressions of circIL21R, miR-1205, and PTBP1 were tested via qRT-PCR.

Xenograft experiments

5 weeks old female BALB/c-nude mice were raised at the Capital Medical University. We set two groups randomly as circIL21R-OE and circIL21R-EV. As for subcutaneous tumor injection, circIL21R overexpression plasmid transfected ME180 cell lines. Tumor growth was monitored every day. Samples were harvested and weighed after euthanizing mice 3 weeks after the injection. This research used the formula $(D \times d^2)/2$ to calculate the tumor size (D and d represent the sample's long and short diameter). All animal experiments were performed according to the ethics of the Capital Medical University.

Immunohistochemistry (IHC)

IHC staining of animal xenograft tumor samples was conducted as previously described [22]. The thickness of paraffin-embedded tumor sample slides was 4 μm. Primary antibodies labeled samples against PTBP1 and ki-67 (ab15580, Abcam). An optical microscope (Olympus) acquired IHC images.

Bioinformatic analyses

The expression of circIL21R in cervical cancer was acquired from Gene Expression Omnibus (GEO) datasets GSE109569 and the detailed data is shown in Supplementary Table 1. Datasets of Targetscan, miRWalk, miRDB, and miRPathDB were used to explore the correlations between circIL21R, miR-1205, and PTBP1. We validate the binding sites between circIL21R, miR-1205, and PTBP1 through Starbase (starbase.sysu.edu.cn) dataset.

Statistical analysis

SPSS 21.0 software (SPSS Inc., Chicago, IL, USA) was conducted for statistical analysis. Student's t-test or one-way variance analysis (ANOVA) calculated differences among various groups. The Log-rank test and Kaplan-Meier analysis were performed to analyze the survival results of patients. *$P < 0.05$ was considered a statistically significant difference. All experiments were repeated 3 times.

Results

CircIL21R expression was upregulated in cervical cancer

The selection of target circRNAs was based on the GEO dataset (GSE102686). We excluded all circRNAs already studied and then selected the

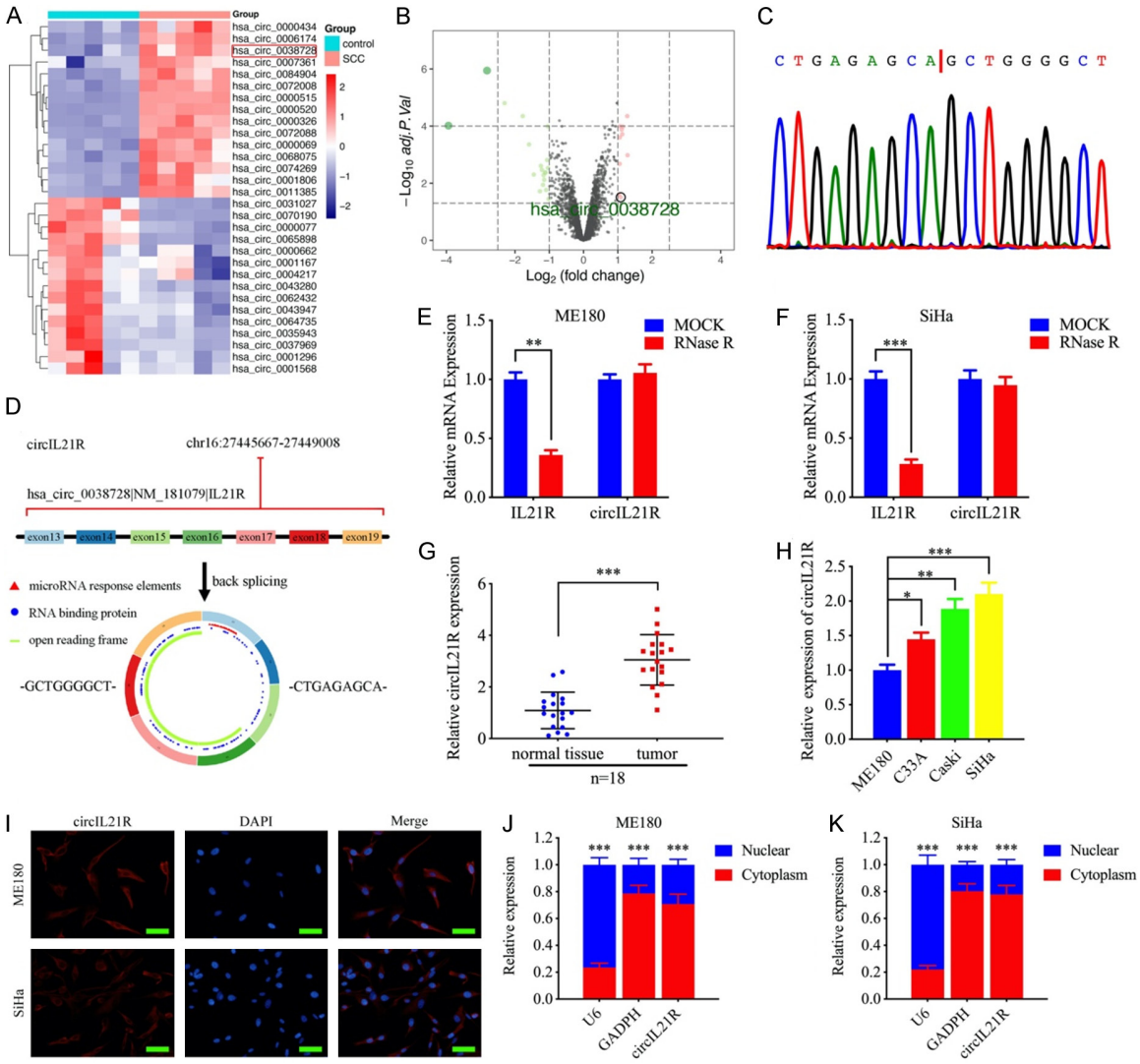

Figure 1. CircIL21R expression was upregulated in cervical cancer. A: Heatmap showing that circIL21R was markedly more highly expressed in cervical cancer tissue than in normal tissue in the GSE109569 dataset. B: The volcano plot demonstrated that circIL21R was highly expressed in cervical cancer. C: Sanger sequencing confirmed the head-to-tail splicing of circIL21R. D: The process of loop formation for circIL21R is described. E, F: Relative RNA expression between IL21R and CircIL21R in ME180 and SiHa cells subjected to RNase R digestion was tested by qPCR. G: CircIL21R was expressed at a greater level in tumor tissue than in adjacent normal tissues, as determined by qPCR. H: A gradient distribution of circIL21R expression levels across the four cell lines was detected by qPCR. I: FISH assays in ME180 and SiHa cells showed the cellular localization of circIL21R using a specific circIL21R probe. Scale bar = 50 μm. J, K: Nuclear-cytoplasmic fractionation assays in ME180 and SiHa cells revealed that circIL21R is primarily located in the cytoplasm. All the data are expressed as the means ± SDs (of three independent experiments). *P < 0.05; **P < 0.01; ***P < 0.001.

3 top circRNAs based on limma differential gene expression analysis to perform qPCR analysis in 18 patient samples. The results showed that hsa_circ_0038728 (circIL21R) had the highest differential expression between tumor tissue and adjacent normal tissue (Supplementary Figure 1). Therefore, we decided to choose this gene as the target for our study. First, bioinformatics analysis revealed that the expression level of circIL21R in cervical cancer tissue was significantly greater than that in normal tissue (**Figure 1A**, **1B**). The loop structure of hsa_circ_0038728 (circIL21R) originated from transcript 16 of IL21R (chr16:27445667-27449008) and was validated by Sanger sequencing (**Figure 1C**, **1D**). RNase R assays showed that the mRNA expression of IL21R was considerably downregulated

in the ME180 and SiHa cell lines after RNase R treatment compared to that in the circIL21R group, confirming that RNase R could not digest circIL21R (**Figure 1E**, **1F**). Eighteen clinical specimens were collected to verify the results of the bioinformatics analysis via qPCR assays. CircIL21R expression was significantly greater in tumor tissue than in adjacent normal tissue (**Figure 1G**). **Figure 1G** shows the expression level of circIL21R in four different cell lines as determined by qPCR (**Figure 1H**). Moreover, FISH was performed in ME180 and SiHa cells to determine the cellular localization of circIL21R in the cytoplasm (**Figure 1I**). Nuclear-cytoplasmic fractionation assays in ME180 and SiHa cells also confirmed that circIL21R was located mainly in the cytoplasm (**Figure 1J**, **1K**). In summary, circIL21R is a potential biomarker related to the progression of cervical cancer and poor survival time.

CircIL21R overexpression promoted cervical cancer cell proliferation and invasion

To study the possible function of circIL21R in cervical cancer cells, we used four cell lines: ME180, C33A, Caski, and SiHa, for follow-up experiments. qPCR assays were used to determine the relative mRNA expression of circIL21R (**Figure 1H**). Lentivirus-coated circIL21R overexpression plasmids were designed and used to infect ME180 and C33A cells to conduct gain-of-function assays, and the infection efficiency was tested by qPCR (**Figure 2A**, **2B**). We first performed MTS assays and found that the absorbance of ME180 and C33A cells in the overexpression group was greater than that in the empty vector (EV) group, which indicated that overexpression of circIL21R can increase the viability of tumor cells (**Figure 2C**, **2D**). EdU assays were subsequently used to test the proliferative capacity of tumors overexpressing circIL21R. Compared with those in the EV group, there was a marked increase in the number of EdU-positive cells after circIL21R overexpression (**Figure 2E**, **2F**). Transwell assays were used to measure the invasion of tumor cells, and we found that circIL21R-overexpressing ME180 and C33A cells had greater potential than circIL21R-EV cells (**Figure 2G**, **2H**).

CircIL21R served as a sponge for miR-1205

As previously stated, circRNAs contain many miRNA response elements (MREs) that sponge miRNAs, mediate the expression of miRNAs that target downstream genes, and perform various physiological and pathological functions [23]. Identification of the downstream target of circIL21R is necessary to elucidate its cancer-promoting mechanisms after validating that upregulating the expression level of circIL21R can promote the malignant phenotypes of cervical cancer. Therefore, the circInteractome and circBANK datasets were used to identify the potential target miRNAs of circIL21R, and there were two overlapping miRNAs, miR-571 and miR-1205, as shown in **Figure 3A**. qPCR assays after circIL21R overexpression and knockdown verified that miR-1205 had a greater effect on the change in the expression of circIL21R (**Figure 3C**, **3D**). We chose to perform further experiments, and **Figure 3B** shows the binding site of circIL21R to miR-1205. qPCR assays of the 18 clinical specimens revealed that miR-1205 expression was significantly greater in adjacent normal tissue than in tumor tissue (**Figure 3E**). Moreover, we validated that upregulating and downregulating miR-1205 can also inversely regulate the expression of circIL21R via qPCR in cell lines (**Figure 3F**, **3G**). Luciferase reporter assays further revealed that the luciferase activity of wild-type circIL21R increased in ME180 and C33A cells after miR-1205 inhibitor treatment, while statistically significant changes were not detected in the mt-type cells (**Figure 3H**, **3I**). Additionally, the luciferase activity of wild-type circIL21R decreased in Caski and SiHa cells after miR-1205 mimic treatment, while that of mt-type cells did not significantly differ (**Figure 3J**, **3K**). Because miRNAs frequently function through the RNA-induced silencing complex (RISC) and because the AGO2 protein is a critical component of the RISC [24], we used anti-AGO2 RIP assays to test the enrichment of miR-1205 and circIL21R in SiHa cells. The pull-down efficiency of the anti-AGO2 antibodies was satisfactory compared to that of the IgG group. Furthermore, circIL21R and miR-1205 were strongly enriched after miR-1205 mimic treatment compared to those in the negative control (NC) group (**Figure 3L**, **3M**). The results above suggested that miR-1205 was a possible downstream target of circIL21R.

CircIL21R overexpression promoted the progression of cervical cancer cells via miR-1205

We then conducted MTS assays, EdU assays, and Transwell assays as a series of rescue

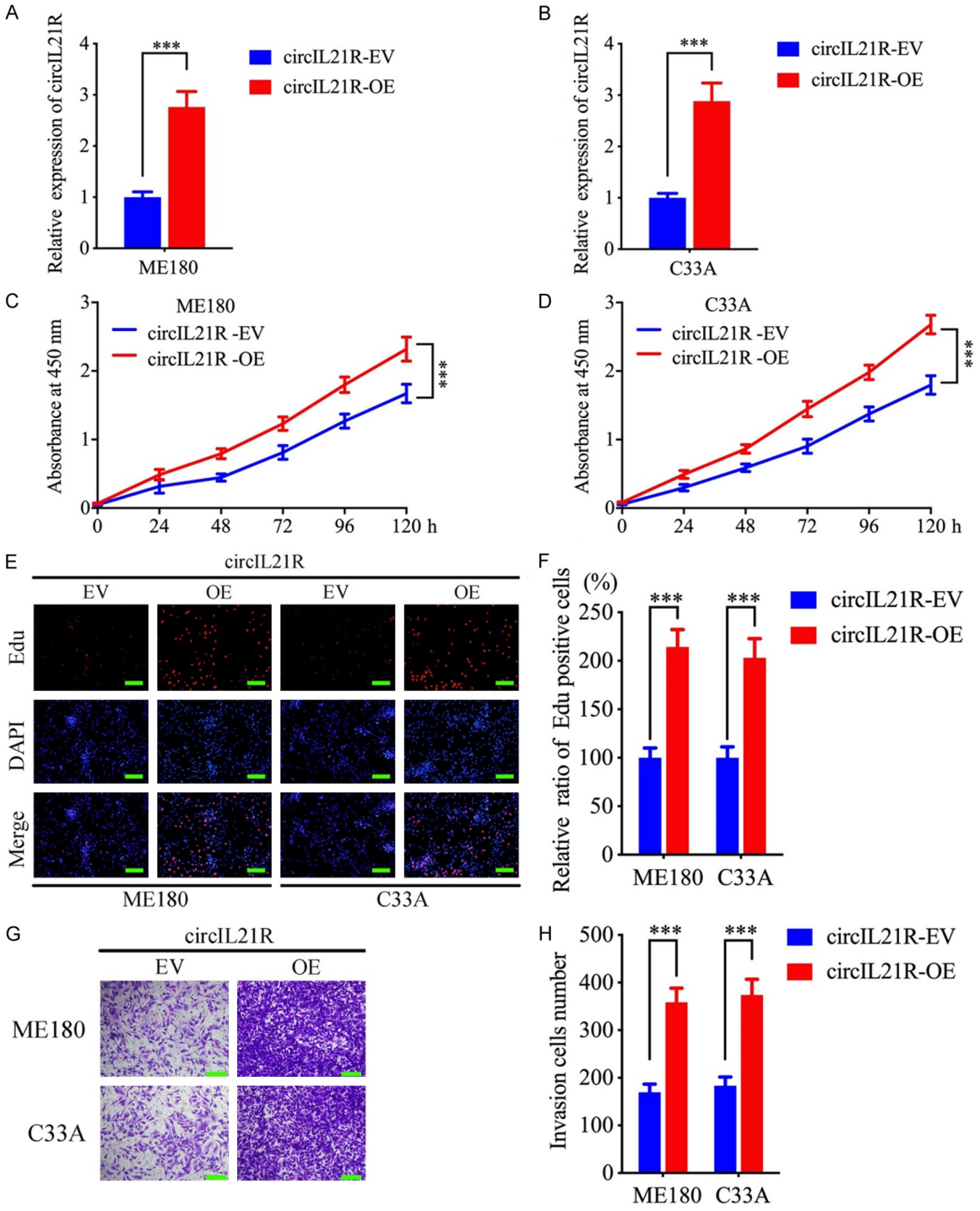

Figure 2. Overexpression of circIL21R promoted cervical cancer cell proliferation and invasion. A, B: qPCR analysis of the overexpression efficiency of ME180 and C33A. C, D: MTS assays showed that the viability of ME180 and C33A cells increased after circIL21R overexpression. E, F: EdU assays revealed an increase in the proliferation of ME180 and C33A cells following circIL21R overexpression. Scale bar = 100 μm. G, H: Transwell assays were used to determine the increase in invasion ability of cervical cancer cells after circIL21R overexpression. Scale bar = 100 μm. All the data are expressed as the means ± SDs (of three independent experiments). *P < 0.05; **P < 0.01; ***P < 0.001.

experiments to explore whether the expression of miR-1205 can mediate the tumor-promoting effects of circIL21R. In the MTS assays, circIL21R overexpression in ME180 and C33A

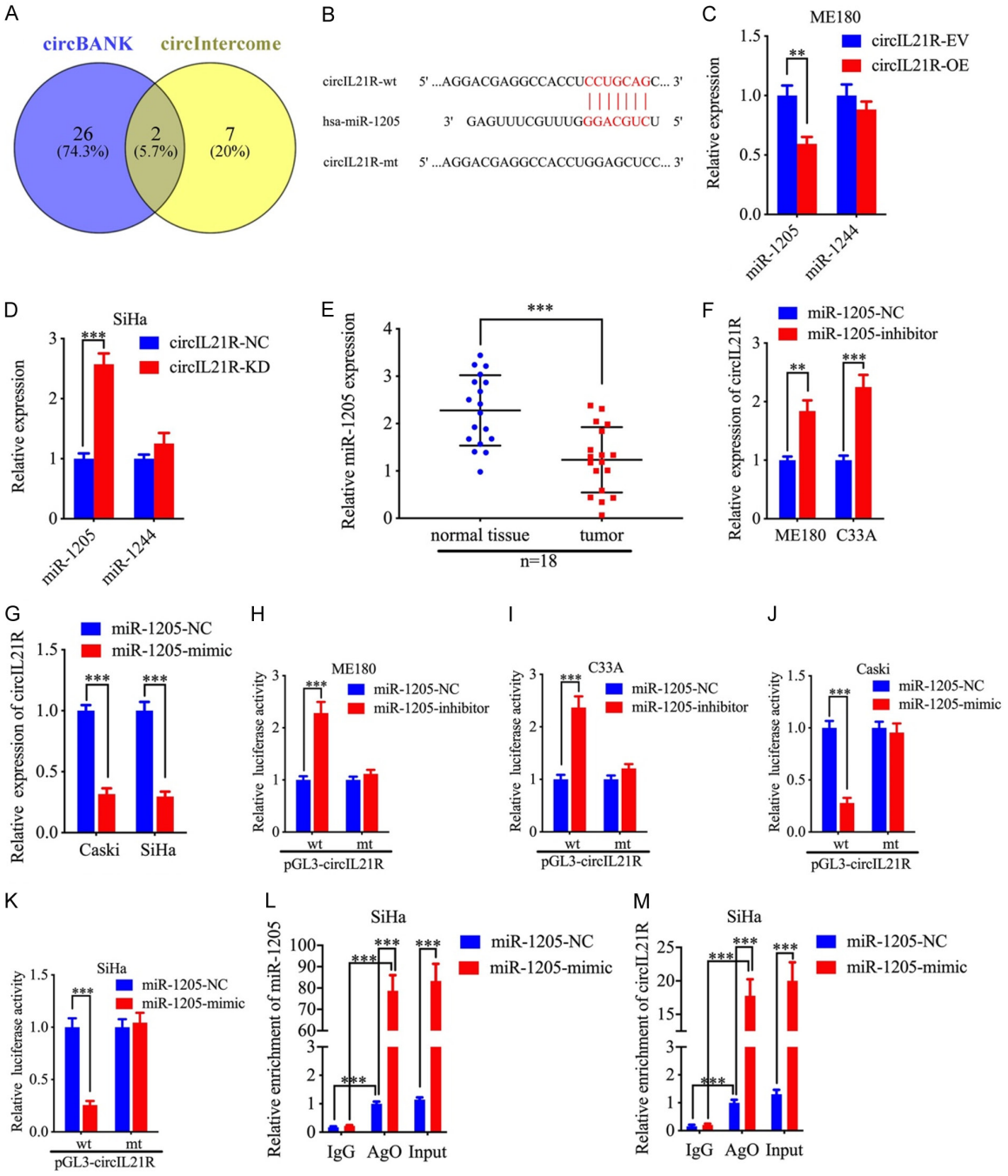

Figure 3. CircIL21R served as a sponge for miR-1205. A: Venn diagram showing the intersection of the circIntercome and circBANK databases that predicted the two potential target miRNAs of circIL21R. B: Diagram of the binding site of circIL21R to miR-1205. C, D: qPCR assays confirmed that the overexpression of miR-1205 in ME180 cells and the knockdown of miR-1205 in SiHa cells resulted in a more significant change in miR-1205 expression than in miR-1244 expression. E: qPCR assays showed that the relative expression of miR-1205 was lower in tumor tissue than in adjacent normal tissue. F, G: qPCR assays illustrated that miR-1205-inhibitor treatment (ME180 and C33A) and miR-1205-mimic treatment (Caski and SiHa) reversely regulated the expression of circIL21R. H-K: Luciferase reporter gene assays showed that miR-1205 inhibitor treatment (ME180 and C33A) and miR-1205 mimic treatment (Caski and SiHa) altered the luciferase activity of circIL21R. L, M: RIP assays demonstrated that miR-1205 and circIL21R were effectively pulled down by anti-AGO2 antibodies compared with IgG and were enriched after mimic treatment with miR-1205 in SiHa cells. All the data are expressed as the means ± SDs (of three independent experiments). *P < 0.05; **P < 0.01; ***P < 0.001.

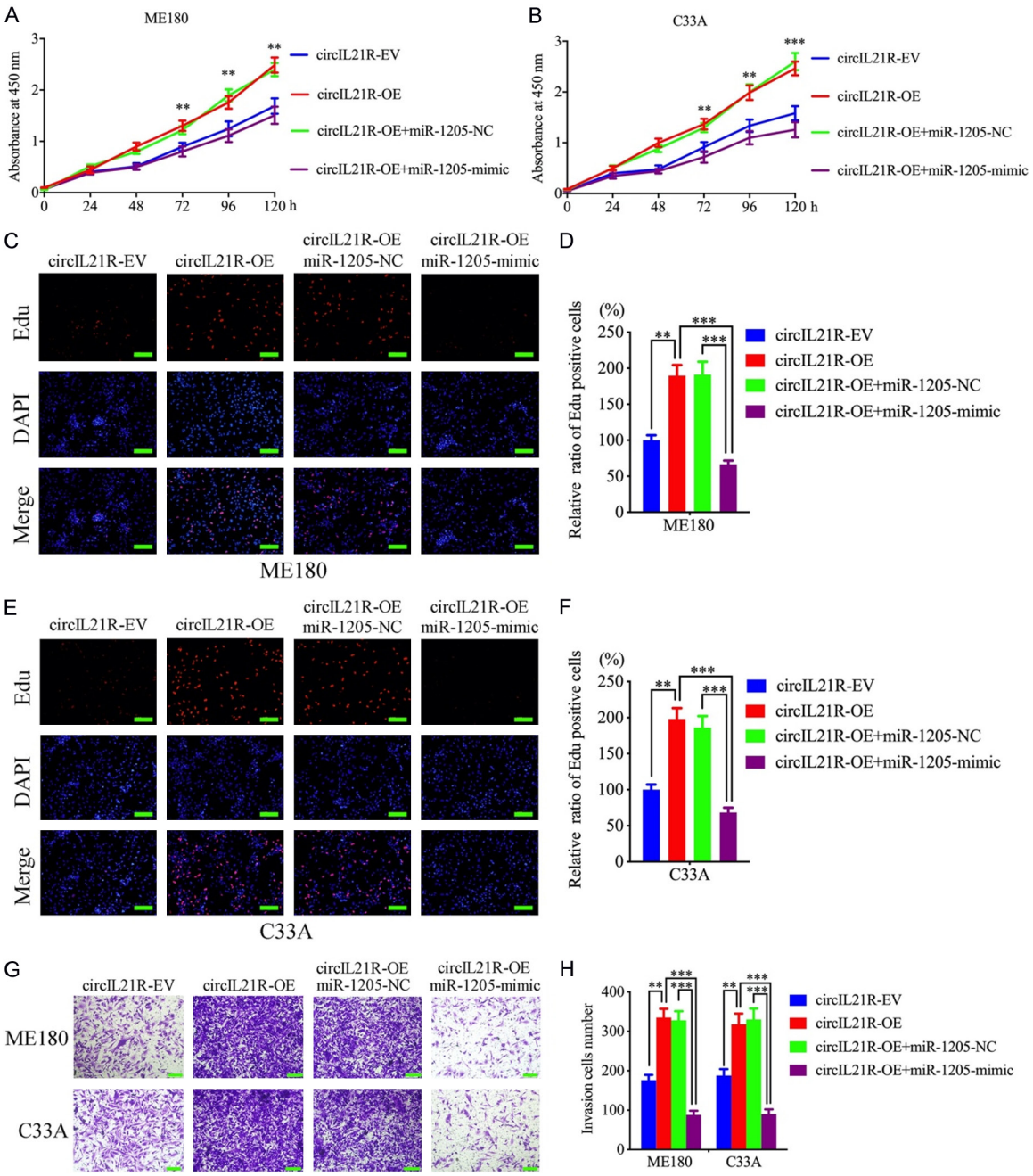

Figure 4. Overexpression of circIL21R promoted cervical cancer progression via miR-1205. A, B: MTS assays showed that the increase in absorbance caused by circIL21R overexpression decreased after miR-1205 mimic treatment in ME180 and C33A cells. C-F: EDU assays confirmed that miR-1205 mimic treatment reversed the proliferation-promoting effect of circIL21R overexpression in ME180 and C33A cells. Scale bar = 100 μm. G, H: Transwell assays confirmed that miR-1205 mimic treatment offset the enhanced invasion capacity caused by circIL21R overexpression in ME180 and C33A cells. Scale bar = 100 μm. All the data are expressed as the means ± SDs (of three independent experiments). *P < 0.05; **P < 0.01; ***P < 0.001.

cells increased the absorbance value on a large scale, but the value decreased significantly after miR-1205 mimic treatment (**Figure 4A**, **4B**). EdU assays showed that the increase in the percentage of EdU-positive cells caused by circIL21R overexpression decreased markedly after miR-1205 mimic treatment in ME180 and C33A cells (**Figure 4C-F**). Transwell assays

showed similar results. circIL21R overexpression enhanced the invasion capacity of ME180 and C33A tumor cells. However, miR-1205 mimic treatment excessively suppressed the invasion-promoting effect (**Figure 4G**, **4H**). These results strongly revealed the mechanism by which miR-1205 negatively regulates the tumor-promoting function of circIL21R in cervical cancer.

PTBP1 is a downstream target oncogene of miR-1205

Using four datasets, TargetScan, miRWalk, miRDB, and miRPathDB, we identified two possible downstream oncogenes related to miR-1205: PTBP1 and SBNO1 (**Figure 5A**). Then, qPCR assays were used to identify the most effective target. Only the expression of PTBP1 was upregulated after miR-1205 inhibitor treatment in ME180 cells and downregulated after miR-1205 mimic treatment in SiHa cells (**Figure 5B**, **5C**). **Figure 5D** illustrates the binding site of the target oncogene between miR-1205 and PTBP1. We next performed a series of bioinformatics analyses to determine the oncogenic role of PTBP1 in cervical cancer. The TCGA dataset showed that the expression of PTBP1 in cervical cancer tissue was much greater than that in normal tissue (**Figure 5E**). Kaplan-Meier survival curve analysis verified that patients with higher PTBP1 expression had poorer survival than those with lower PTBP1 expression (**Figure 5F**). The receiver operating characteristic (ROC) curve also showed that PTBP1 was an effective diagnostic biomarker of cervical cancer (**Figure 5G**). Luciferase reporter assays confirmed that miR-1205 inhibitor treatment upregulated the luciferase activity of ME180 and C33A cells in the PTBP1-wt group compared with that in the PTBP1-mt group (**Figure 5H**, **5I**). In contrast, miR-1205 mimic treatment downregulated the luciferase activity of the PTBP1-wt group, while no significant difference was observed after treatment in the PTBP1-mt group (**Figure 5J**, **5K**). We also used western blotting to verify whether miR-1205 can mediate the expression of PTBP1. The results showed that PTBP1 expression increased with miR-1205 inhibitor treatment in ME180 cells, while the opposite trend was observed after miR-1205 mimic treatment in SiHa cells (**Figure 5L**).

CircIL21R regulated PTBP1 expression via miR-1205

Western blot and qPCR assays revealed that the overexpression of circIL21R upregulated the expression of PTBP1 at both the mRNA and protein levels. However, miR-1205 mimic treatment reversed these effects (**Figure 6A-C**). A series of phenotype experiments were designed to validate whether circIL21R could promote the malignant behaviors of cervical cancer cell lines by upregulating PTBP1 through a miR-1205-mediated mechanism. MTS (**Figure 6D**, **6E**), EDU (**Figure 6F-H**), and Transwell (**Figure 6I**, **6J**) assays revealed that circIL21R overexpression in ME180 and C33A cells significantly increased cell viability, proliferation, and invasion capacity. In the next step, we conducted additional PTBP1 knockdown on the basis of circIL21R overexpression. We observed that the tumorigenic effects produced by circIL21R overexpression were reversed. In summary, these results effectively suggested that circIL21R plays an essential role in regulating PTBP1 expression via a miR-1205-mediated mechanism and promoting the progression of cervical cancer.

SFRS1 directly binds to circIL21R to maintain its stability and upregulate its expression in cervical cancer

RNA binding proteins (RBPs) play a crucial role in maintaining the stability and regulating the functions of circRNAs based on their back-splicing ability [25, 26]. We explored RBPsuite (http://www.csbio.sjtu.edu.cn/bioinf/RBPsuite/) to identify the potential RBPs that significantly influence circIL21R and lead to its overexpression in cervical cancers. According to the dataset, 35 candidate RBPs were predicted and are listed in **Figure 7A** in order of their binding score (**Figure 7A**). The top five candidate RBPs were selected for verification by qPCR. SFRS1 was the only circRNA that upregulated the expression of circIL21R after overexpression in ME180 cells but downregulated it after knockdown in SiHa cells (**Figure 7B**, **7C**). **Figure 7D** shows the binding score between SFRS1 and circIL21R (**Figure 7D**). In subsequent RIP assays, the results indicated that anti-SFRS1 treatment increased the expression of circIL21R compared to IgG treatment. Moreover, the enrichment of circIL21R increased or decreased upon overexpression or knockdown

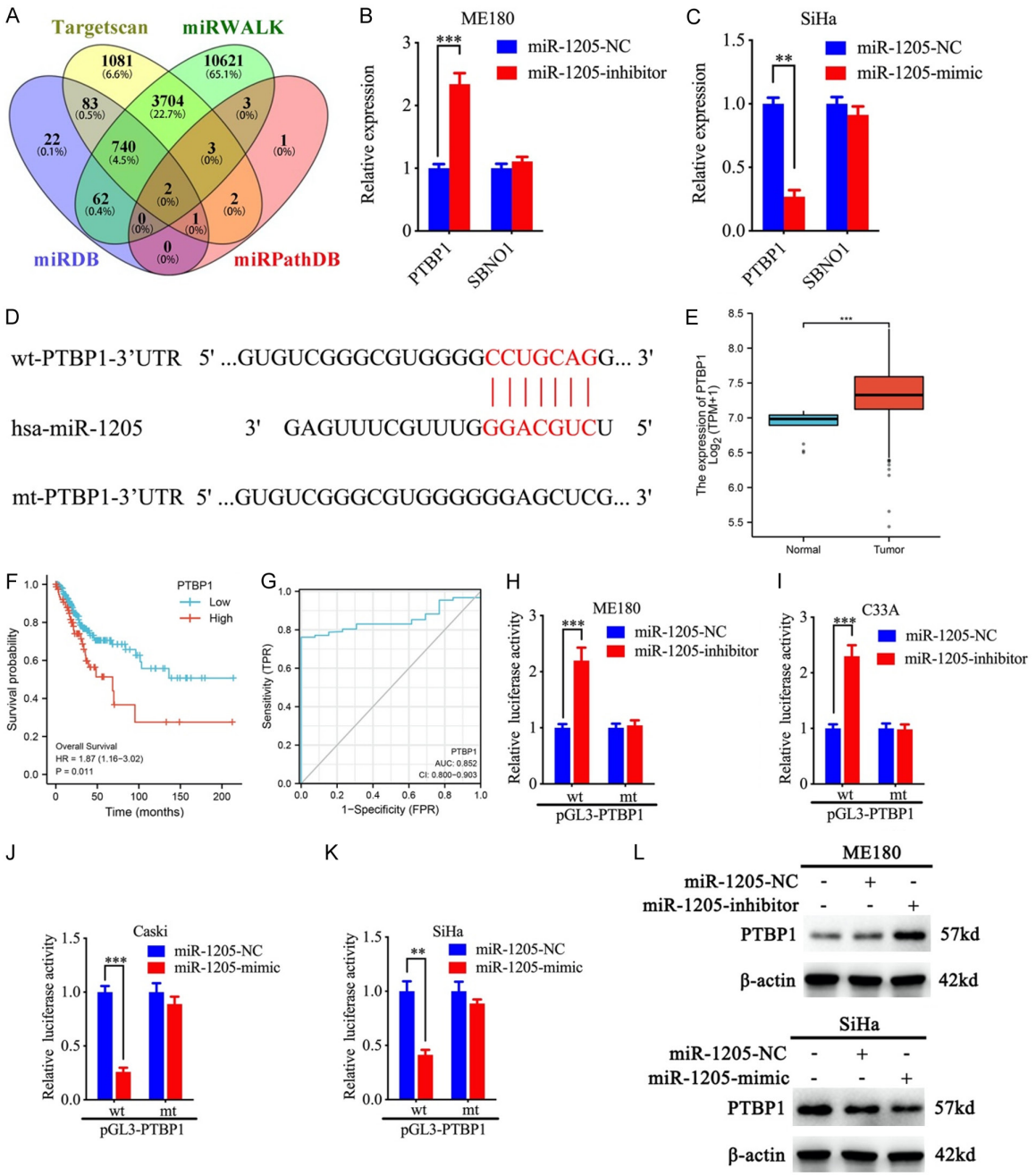

Figure 5. PTBP1 is a downstream target oncogene of miR-1205. A: Venn diagram illustrating an intersection of four databases that predicted the two potential target oncogenes of miR-1205. B, C: qPCR assays confirmed that miR-1205-inhibitor treatment in ME180 cells and miR-1205-mimic treatment in SiHa cells resulted in a more significant change in PTBP1 expression than in SBNO1 expression. D: Diagram of the binding site of miR-1205 in PTBP1. E: The expression of PTBP1 in cervical cancer tissue was greater than that in normal tissue based on the TCGA dataset. F: Kaplan-Meier survival analysis revealed that cervical cancer patients with lower PTBP1 expression had better survival outcomes than those with higher PTBP1 expression. G: ROC curve analysis indicated that PTBP1 was an effective diagnostic biomarker of cervical cancer. H-K: Luciferase reporter gene assays demonstrated that miR-1205 inhibitor treatment (ME180 and C33A) and miR-1205 mimic treatment (Caski and SiHa) regulated the luciferase activity of PTBP1. L: Western blotting showing the expression of PTBP1 after miR-1205 inhibition in ME180 cells and mimic treatment in SiHa cells. All the data are expressed as the means ± SDs (of three independent experiments). *P < 0.05; **P < 0.01; ***P < 0.001.

of circIL21R, respectively, in response to anti-SFRS1 treatment (**Figure 7E-H**). Furthermore, we investigated whether SFRS1 can maintain its stability and upregulate the expression

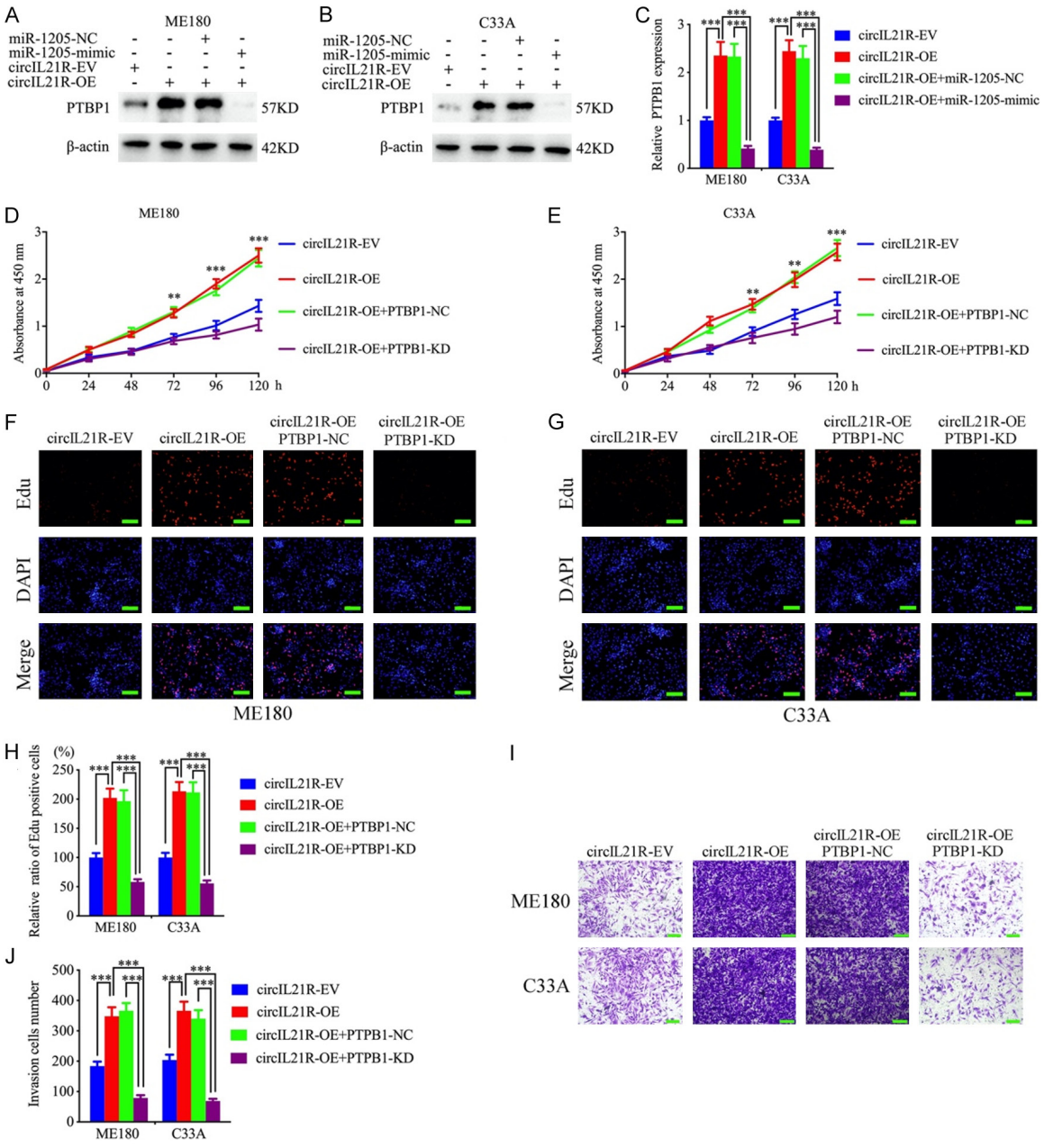

Figure 6. CircIL21R regulated PTBP1 expression via miR-1205. A-C: Western blotting and qPCR assays revealed that the increase in PTBP1 expression induced by circIL21R overexpression was reversed after miR-1205 mimic treatment in ME180 and C33A cells. D, E: MTS assays demonstrated that the increase in viability of ME180 and C33A cells promoted by circIL21R overexpression was reversed after PTBP1 knockdown. F-H: The EdU assay revealed that the increased proliferation of ME180 and C33A cells caused by circIL21R overexpression was reversed after PTBP1 knockdown. Scale bar = 100 μm. I, J: Transwell assays revealed that PTBP1 knockdown inhibited the enhanced tumor invasion capacity induced by circIL21R overexpression in ME180 and C33A cells. Scale bar = 100 μm. All the data are expressed as the means ± SDs (of three independent experiments). *P < 0.05; **P < 0.01; ***P < 0.001.

of circIL21R. RNA stability assays revealed that SFRS1 overexpression significantly prolonged the half-life of circIL21R compared to that of the negative control in ME180 and C33A cells (**Figure 7I**, **7J**). In summary, SFRS1 is a promising RBP that can directly bind to circIL21R, thereby maintaining its stability and upregulating its expression.

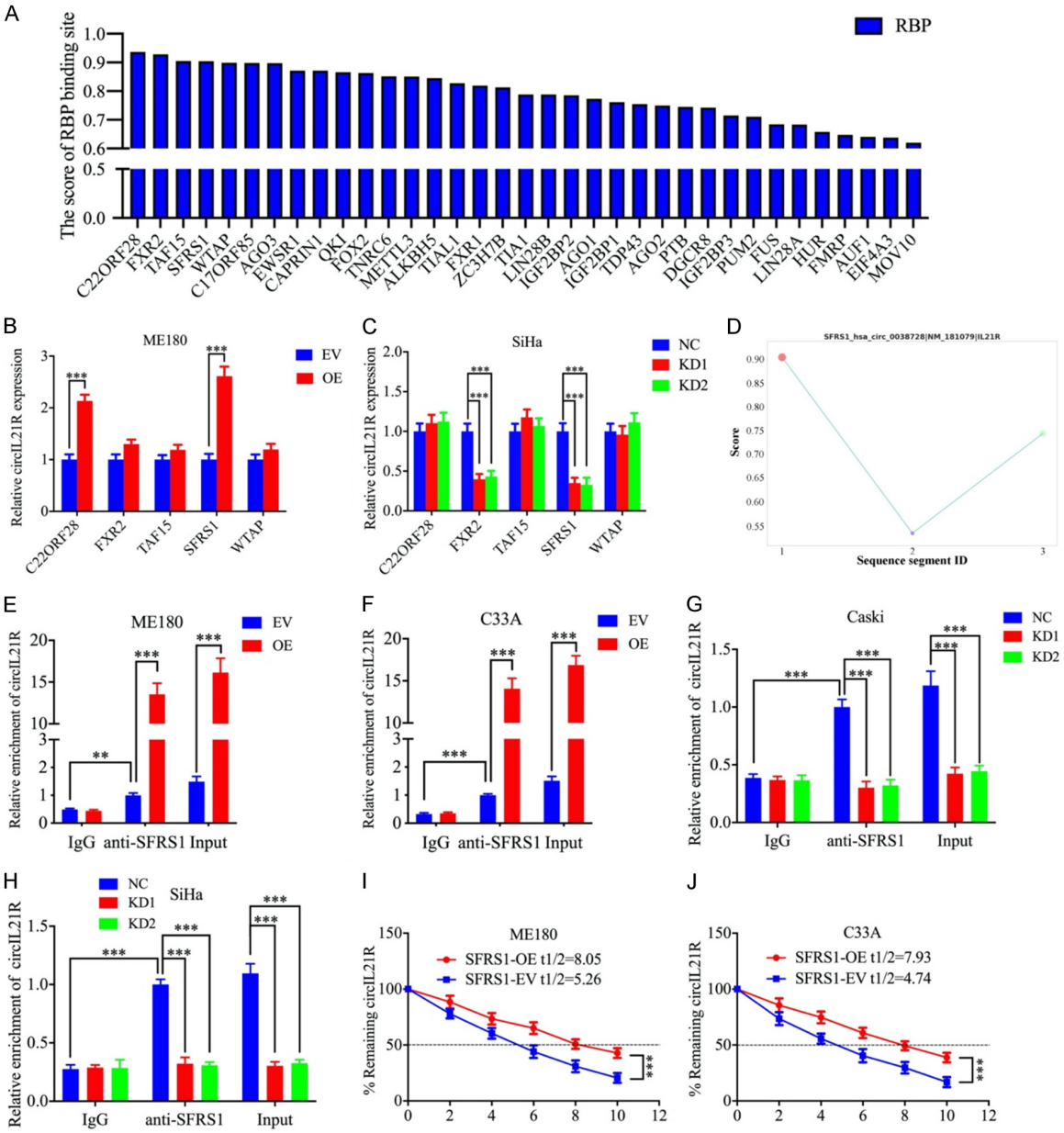

Figure 7. SFRS1 directly binds to circIL21R to maintain its stability and upregulate its expression in cervical cancer. A: The binding score of RBPs with a binding site for circIL21R. B, C: qPCR confirmed that SFRS1 is the only RBP that regulates the expression of circIL21R after both ME180 knockdown and SiHa overexpression. D: Diagram of the binding score between SFRS1 and circIL21R. E-H: RIP assays demonstrated that circIL21R was effectively pulled down by anti-SFRS1 antibodies compared with IgG, and the enrichment was greater after SFRS1 overexpression (ME180 and C33A) or lower after SFRS1 knockdown (Caski and SiHa). I, J: RNA stability assays illustrated that the remaining expression levels of circIL21R were greater in the SFRS1-overexpressing group than in the EV group. All the data are shown as the means ± SDs (of three independent experiments). *P < 0.05; **P < 0.01; ***P < 0.001.

CircIL21R overexpression promoted cervical cancer growth in vivo

Cervical cancer xenograft models were established to explore the function of circIL21R in vivo. Overexpression of circIL21R led to a significant increase in tumor volume and weight in ME180 mice (**Figure 8A**, **8B**). Further hematoxylin and eosin (H&E) staining, immunohistochemical staining, and qPCR showed that the staining intensity and expression levels of circIL21R, PTBP1, and ki-67 were substantially

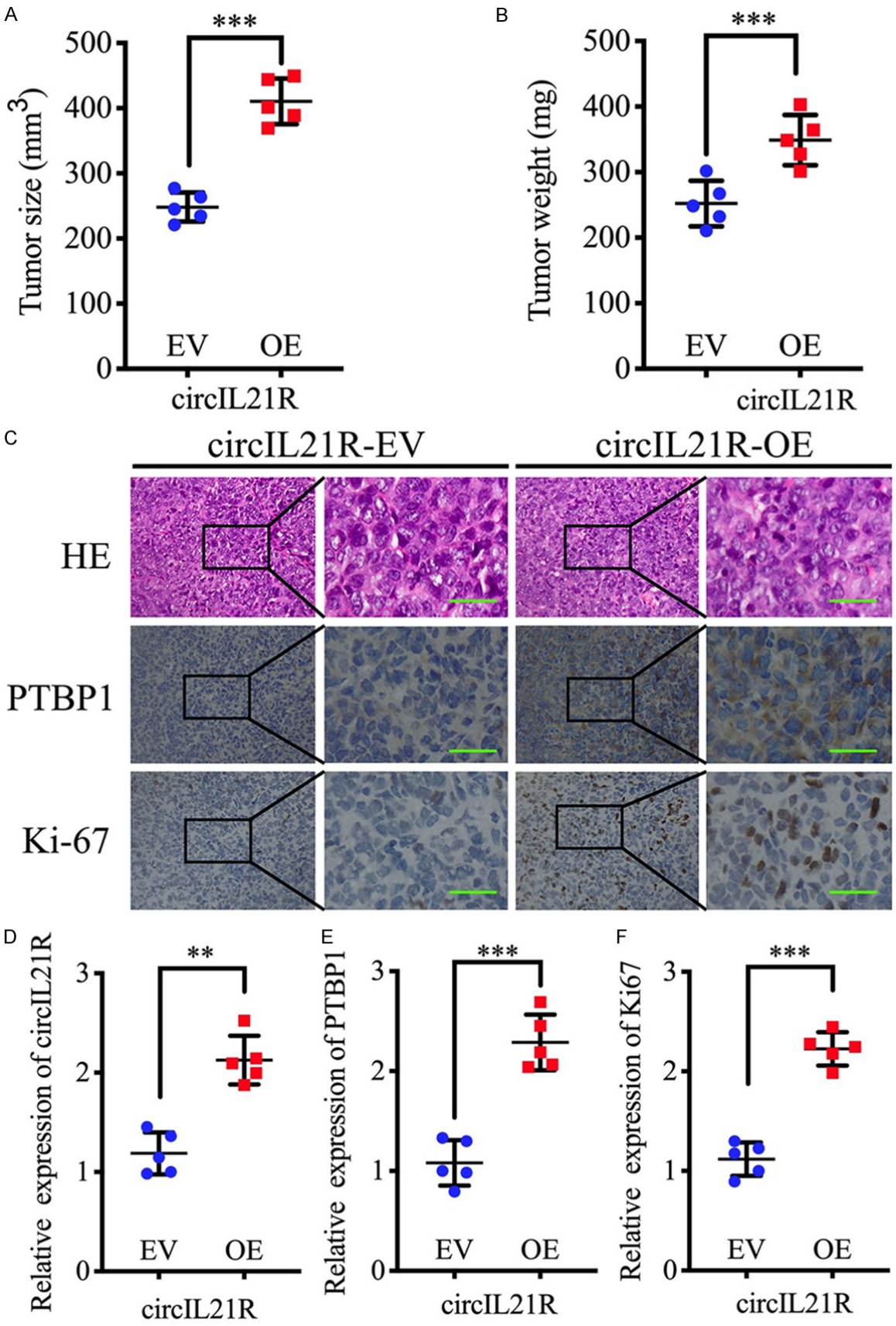
A
***
Tumor size (mm3)
500
400
300
200
100
0
EV
OE
circIL21R
B
***
Tumor weight (mg)
500
400
300
200
100
0
EV
OE
circIL21R
C
circIL21R-EV
circIL21R-OE
HE
PTBP1
Ki-67
D
**
Relative expression of circIL21R
3
2
1
0
EV
OE
circIL21R
E
***
Relative expression of PTBP1
3
2
1
0
EV
OE
circIL21R
F
***
Relative expression of Ki67
3
2
1
0
EV
OE
circIL21R

Figure 8. CircIL21R overexpression promoted cervical cancer growth in vivo. A, B: CircIL21R overexpression significantly enhanced tumor volume and weight. C: H&E staining and immunohistochemical staining showing the expression of circIL21R, PTBP1, and Ki-67 in the circIL21R-EV and circIL21R-OE groups. D-F: qPCR assays confirmed that the circIL21R-OE group had greater expression of circIL21R, PTBP1, and Ki-67 than the circIL21R-EV group. All the data are expressed as the means ± SDs (of three independent experiments). *P < 0.05; **P < 0.01; ***P < 0.001.

greater in the circIL21R-overexpressing group than in the control group (**Figure 8C-F**). These results demonstrated that circIL21R promoted the tumorigenesis of cervical cancer in vivo.

Discussion

Cervical cancer, including squamous, adenocarcinoma, adenosquamous, and small cell carcinoma, is one of the most common malignancies in women, and squamous carcinoma is the most common histological type. Various oncogenic factors can lead to the occurrence and development of cervical cancer by acting on oncogenes. Identifying oncogenes associated with the occurrence and development of cervical cancer can aid in understanding and predicting cervical cancer risk. Moreover, innovative ideas for molecularly targeted therapy can be proposed based on these studies [8].

With the completion of the Human Genome Project, it is now known that less than 2% of all nucleic acid sequences in the human genome can encode proteins, and the vast majority of genes in the human genome are noncoding RNAs, such as long noncoding RNAs, miRNAs, and circRNAs [27]. However, due to the short period of discovery and the limitations of previous experimental techniques, the role of massive amounts of noncoding RNA molecules in the physiological and pathophysiological processes of the organism is poorly understood [28]. In particular, although circRNAs were discovered as early as the 1970s, their exact biological mechanisms of action were not known until the last decade. Increasingly, studies have shown that dysregulation of circRNAs is positively correlated with clinical progression in tumor patients and has become a hot topic of current research [29].

In this study, GEO analysis revealed a new circRNA, termed circIL21R, whose expression is distinctly greater in cervical cancer tissue than in normal tissue. Moreover, the expression level of circIL21R was negatively correlated with patient survival. RNase R was used to visualize the circular structures of circIL21R in cell lines before further gain-of-function assays were performed to analyze the function of circIL21R in the course of cervical cancer. The results showed that high expression of circIL21R strongly promoted proliferation and growth but suppressed apoptosis in cancer cells, illustrating that circIL21R plays a vital role in promoting the development of cervical cancer.

Several meaningful reports have demonstrated that circRNAs may regulate the downstream targets of miRNAs by acting as competing endogenous RNAs (ceRNAs) to suppress miRNAs [30]. For example, circZMYM4 overexpression suppressed the proliferation and metastasis of lung cancer cells, while overexpression of miR-587 reversed these effects [31]. CircASPM, which upregulated the growth and proliferation of glioblastoma both in vitro and in vivo, modulated PTBP1 at a relatively high level by sponging miR-130b-3p [21]. This research explored two potential miRNAs by bioinformatic analysis and validated miR-1205 as a target of circIL21R. Subsequent experiments demonstrated that the expression of miR-1205 was inversely correlated with that of circIL21R and that miR-1205 mimic treatment weakened the tumor-promoting effects caused by circIL21R overexpression.

PTBP1 is a crucial functional gene that mediates many cellular processes and is expressed in almost every cell type. Its function can be regulated by several molecules, including long noncoding RNAs, miRNAs, and some RNA-binding proteins [32]. In this study, we found that PTBP1 was the downstream target of miR-1205. Nevertheless, the results demonstrated that circIL21R overexpression could upregulate PTBP1 protein mRNA levels in cervical cancer cell lines. Moreover, PTBP1 knockdown reversed the tumor-promoting effects caused by circIL21R overexpression, illustrating that circIL21R regulated the expression of PTBP1 by acting as a ceRNA for miR-1205.

Xenograft experiments were performed to validate the experimental results, and we found

that overexpression of circIL21R increased the weight and volume of tumors in mice. IHC staining of tumor tissue revealed that the expression levels of circIL21R, PTBP1, and ki-67 were upregulated on a large scale compared to those in the control groups. These data proved that circIL21R promotes the tumorigenesis of cervical cancer in vivo. However, further studies are needed to determine the underlying mechanisms involved, such as angiogenesis or signaling pathways.

Conclusion

Our study illustrated that circIL21R is highly expressed in cervical cancers and upregulates PTBP1 expression by acting as a ceRNA for miR-1205, which promotes several malignant biological processes in cervical cancers, such as growth, proliferation, and invasion. circIL21R is a potential biomarker for the diagnosis and treatment of cervical cancer.

Acknowledgements

This work was supported by the Project of National Multidisciplinary Collaborative Diagnosis and Treatment Capacity Building for Major Diseases and the Shanghai Sailing Program (No. 21YF1449900).

Written informed consent was obtained from all patients.

Disclosure of conflict of interest

None.

Abbreviations

circRNAs, circular RNAs; ncRNAs, non-coding RNAs; miRNAs, microRNAs; RBP, RNA-binding protein; PTBP1, polypyrimidine tract-binding protein 1; WHO, World Health Organization; qRT-PCR/qPCR, Real-Time Quantitative Reverse Transcription PCR; RIP, RNA immunoprecipitation; GEO, Gene Expression Omnibus; ANOVA, one-way variance analysis; IHC, Immunohistochemistry; RISC, RNA-induced silencing complex; MREs, microRNA response elements; ceRNAs, competing endogenous RNAs; H&E, hematoxylin and eosin.

Address correspondence to: Jun Zhang and Xiaohui Xu, Department of Obstetrics and Gynecology, Beijing Anzhen Hospital Affiliated to Capital Medical University, Beijing 100011, China. E-mail: drzhangj@outlook.com (JZ); lyb20231216@163.com (XHX)

References

[1] Aitken RJ. Age, the environment and our reproductive future: bonking baby boomers and the future of sex. Reproduction 2013; 147: S1-S11.

[2] Erratum: Global cancer statistics 2018: GLOBOCAN estimates of incidence and mortality worldwide for 36 cancers in 185 countries. CA Cancer J Clin 2020; 70: 313.

[3] Luo L, Luo Q and Tang L. Diagnostic value and clinical significance of MRI and CT in detecting lymph node metastasis of early cervical cancer. Oncol Lett 2020; 19: 700-706.

[4] Hsu W, Liu L, Chen X, Zhang Y and Zhu W. LncRNA CASC11 promotes the cervical cancer progression by activating Wnt/beta-catenin signaling pathway. Biol Res 2019; 52: 33.

[5] Wang HL, Lu X, Yang X and Xu N. Association of MBL2 exon1 polymorphisms with high-risk human papillomavirus infection and cervical cancers: a meta-analysis. Arch Gynecol Obstet 2016; 294: 1109-1116.

[6] Denny L, Boa R, Williamson AL, Allan B, Hardie D, Stan R and Myer L. Human papillomavirus infection and cervical disease in human immunodeficiency virus-1-infected women. Obstet Gynecol 2008; 111: 1380-1387.

[7] Chen X, Chen L, Zhu H and Tao J. Risk factors and prognostic predictors for cervical cancer patients with lung metastasis. J Cancer 2020; 11: 5880-5889.

[8] Adiga D, Eswaran S, Pandey D, Sharan K and Kabekkodu SP. Molecular landscape of recurrent cervical cancer. Crit Rev Oncol Hematol 2021; 157: 103178.

[9] Patop IL, Wüst S and Kadener S. Past, present, and future of circRNAs. EMBO J 2019; 38: e100836.

[10] Memczak S, Jens M, Elefsinioti A, Torti F, Krueger J, Rybak A, Maier L, Mackowiak SD, Gregersen LH, Munschauer M, Loewer A, Ziebold U, Landthaler M, Kocks C, le Noble F and Rajewsky N. Circular RNAs are a large class of animal RNAs with regulatory potency. Nature 2013; 495: 333-338.

[11] Chen Z, Ling K, Zhu Y, Deng L, Li Y and Liang Z. circ0000069 promotes cervical cancer cell proliferation and migration by inhibiting miR-4426. Biochem Biophys Res Commun 2021; 551: 114-120.

[12] Xie H, Wang J and Wang B. Circular RNA Circ_0003221 promotes cervical cancer progression by regulating miR-758-3p/CPEB4 axis. Cancer Manag Res 2021; 13: 5337-5350.

[13] Yuan DD, Jia CD, Yan MY and Wang J. Circular RNA hsa_circ_0000730 restrains cell proliferation, migration, and invasion in cervical cancer through miR-942-5p/PTEN axis. Kaohsiung J Med Sci 2021; 37: 964-972.
[14] Bartel DP. MicroRNAs: genomics, biogenesis, mechanism, and function. Cell 2004; 116: 281-297.
[15] González-Quintana V, Palma-Berré L, Campos-Parra AD, López-Urrutia E, Peralta-Zaragoza O, Vazquez-Romo R and Pérez-Plasencia C. MicroRNAs are involved in cervical cancer development, progression, clinical outcome and improvement treatment response (Review). Oncol Rep 2016; 35: 3-12.
[16] Wang G, Zhang H and Li P. Upregulation of hsa_circRNA_102958 indicates poor prognosis and promotes ovarian cancer progression through miR-1205/SH2D3A axis. Cancer Manag Res 2020; 12: 4045-4053.
[17] Li JJ, Xiong MY, Sun TY, Ji CB, Guo RT, Li YW and Guo HY. CircFAM120B knockdown inhibits osteosarcoma tumorigenesis via the miR-1205/PTBP1 axis. Aging (Albany NY) 2021; 13: 23831-23841.
[18] Zhong W, Bao L, Yuan Y and Meng Y. CircRASSF2 acts as a prognostic factor and promotes breast cancer progression by modulating miR-1205/HOXA1 axis. Bioengineered 2021; 12: 3014-3028.
[19] Fang G, Wu Y and Zhang X. CircASXL1 knockdown represses the progression of colorectal cancer by downregulating GRIK3 expression by sponging miR-1205. World J Surg Oncol 2021; 19: 176.
[20] Cen Y, Zhu T, Zhang Y, Zhao L, Zhu J, Wang L, Xu J, Ding T, Xie X, Wang X and Lu W. hsa_circ_0005358 suppresses cervical cancer metastasis by interacting with PTBP1 protein to destabilize CDCP1 mRNA. Mol Ther Nucleic Acids 2022; 27: 227-240.
[21] Hou D, Wang Z, Li H, Liu J, Liu Y, Jiang Y and Lou M. Circular RNA circASPM promotes the progression of glioblastoma by acting as a competing endogenous RNA to regulate miR-130b-3p/E2F1 axis. J Cancer 2022; 13: 1664-1678.
[22] Jiang Y, Han S, Cheng W, Wang Z and Wu A. NFAT1-regulated IL6 signalling contributes to aggressive phenotypes of glioma. Cell Commun Signal 2017; 15: 54.
[23] Saliminejad K, Khorram Khorshid HR, Soleymani Fard S and Ghaffari SH. An overview of microRNAs: biology, functions, therapeutics, and analysis methods. J Cell Physiol 2019; 234: 5451-5465.
[24] Huang W, Fang K, Chen TQ, Zeng ZC, Sun YM, Han C, Sun LY, Chen ZH, Yang QQ, Pan Q, Luo XQ, Wang WT and Chen YQ. circRNA circAF4 functions as an oncogene to regulate MLL-AF4 fusion protein expression and inhibit MLL leukemia progression. J Hematol Oncol 2019; 12: 103.
[25] Singh A. RNA-binding protein kinetics. Nat Methods 2021; 18: 335.
[26] Shaath H, Vishnubalaji R, Elango R, Kardousha A, Islam Z, Qureshi R, Alam T, Kolatkar PR and Alajez NM. Long non-coding RNA and RNA-binding protein interactions in cancer: experimental and machine learning approaches. Semin Cancer Biol 2022; 86: 325-345.
[27] Dong P, Xu D, Xiong Y, Yue J, Ihira K, Konno Y and Watari H. The expression, functions and mechanisms of circular RNAs in gynecological cancers. Cancers (Basel) 2020; 12: 1472.
[28] Casarotto M, Fanetti G, Guerrieri R, Palazzari E, Lupato V, Steffan A, Polesel J, Boscolo-Rizzo P and Fratta E. Beyond microRNAs: emerging role of other non-coding RNAs in HPV-driven cancers. Cancers (Basel) 2020; 12: 1246.
[29] Tran AM, Chalbatani GM, Berland L, Cruz De Los Santos M, Raj P, Jalali SA, Gharagouzloo E, Ivan C, Dragomir MP and Calin GA. A new world of biomarkers and therapeutics for female reproductive system and breast cancers: circular RNAs. Front Cell Dev Biol 2020; 8: 50.
[30] Thomson DW and Dinger ME. Endogenous microRNA sponges: evidence and controversy. Nat Rev Genet 2016; 17: 272-283.
[31] Yuan DF, Wang HR, Wang ZF, Liang GH, Xing WQ and Qin JJ. CircRNA circZMYM4 inhibits the growth and metastasis of lung adenocarcinoma via the miR-587/ODAM pathway. Biochem Biophys Res Commun 2021; 580: 100-106.
[32] Zhu W, Zhou BL, Rong LJ, Ye L, Xu HJ, Zhou Y, Yan XJ, Liu WD, Zhu B, Wang L, Jiang XJ and Ren CP. Roles of PTBP1 in alternative splicing, glycolysis, and oncogensis. J Zhejiang Univ Sci B 2020; 21: 122-136.

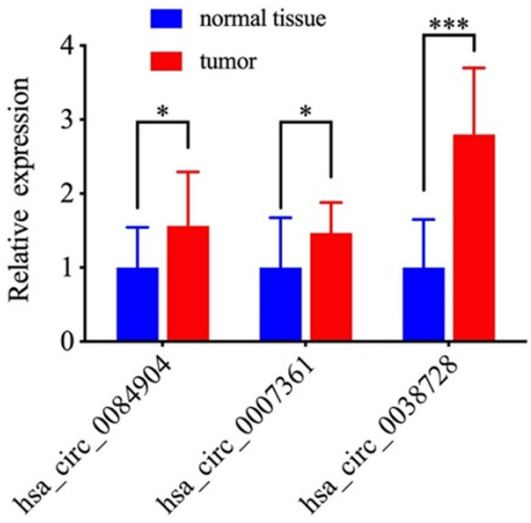

Supplementary Figure 1. Compared with the other two potential circRNAs, hsa_circ_0038728 had the greatest differential expression between tumor and normal tissues. All the data are expressed as the means ± SDs (of three independent experiments). *P < 0.05; **P < 0.01; ***P < 0.001.